Supplementary material

Autoantibodies Targeting a Collecting Duct-specific Water Channel in Tubulointerstitial Nephritis

Nils Landegren*, Mina Pourmousa Lindberg, Jakob Skov, Åsa Hallgren, Daniel Eriksson, Trine Lisberg Toft-Bertelsen, Nanna MacAulay, Eva Hagforsen, Anne Räisänen-Sokolowski, Heikki Saha, Thomas Nilsson, Gunnel Nordmark, Sophie Ohlsson, Jan Gustafsson, Eystein S. Husebye, Erik Larsson, Mark S. Anderson, Jaakko Perheentupa, Fredrik Rorsman, Robert A. Fenton, Olle Kämpe

RESULTS

	Kidney tissue pathology
Patient 1	Representative piece of cortical kidney. There are max. 25 glomeruli, of which 6-8 are completely hyalinized. Other glomeruli are collapsed, atrophic, and there is thickening of Bowman's capsule and pericapsular fibrosis. Tubuli are widely atrophic and the interstitium is fibrotic. There are focal, dense lymphocytic infiltrates. There are no calcifications. The vessels look normal. Conclusion: Chronic interstitial nephritis. Iatrogenic?
Patient 2	The kidney tissue sample does not contain glomeruli. In the small area there are some proximal tubuli that are normal. There are some structural deformities in distal tubuli and collecting tubuli. There is focal PAS- positive amorphic material in the tubuli. The sample is not representative but there is interstitial nephritis and calcification.
Patient 3	The kidney tissue sample has nine glomeruli per section. All glomeruli are open, and two of them have moderate capsular fibrosis. Cellularity of the glomeruli appears slightly increased and matrix is normal. The structure is slightly lobular and the glomeruli are slightly collapsed. Glomeruli basement membranes are normal. There is focal, lymphocytic infiltrates in the interstitium that is occasionally dense. Only few of the infiltrating cells are neutrophils. Tubular structures are partially atrophic and interstitium is fibrotic. There are occasional intraepithelial

	lymphocytes in the tubuli. Some of the tubuli appear primitive. Immunofluoresense: glomeruli are negative for IgG, IgA, IgM, C3, C1q and fibrin. There is some IgM positivity in tubulus epithelium. There are no signs of immunocomplex nephritis. Conlusion: Interstitial nephritis. There is some hypercellularity in the glomeruli.

Table S1. Original pathology reports, translated from Finnish, for the three APS1 patients with tubulointerstitial nephritis and collecting duct autoantibodies.

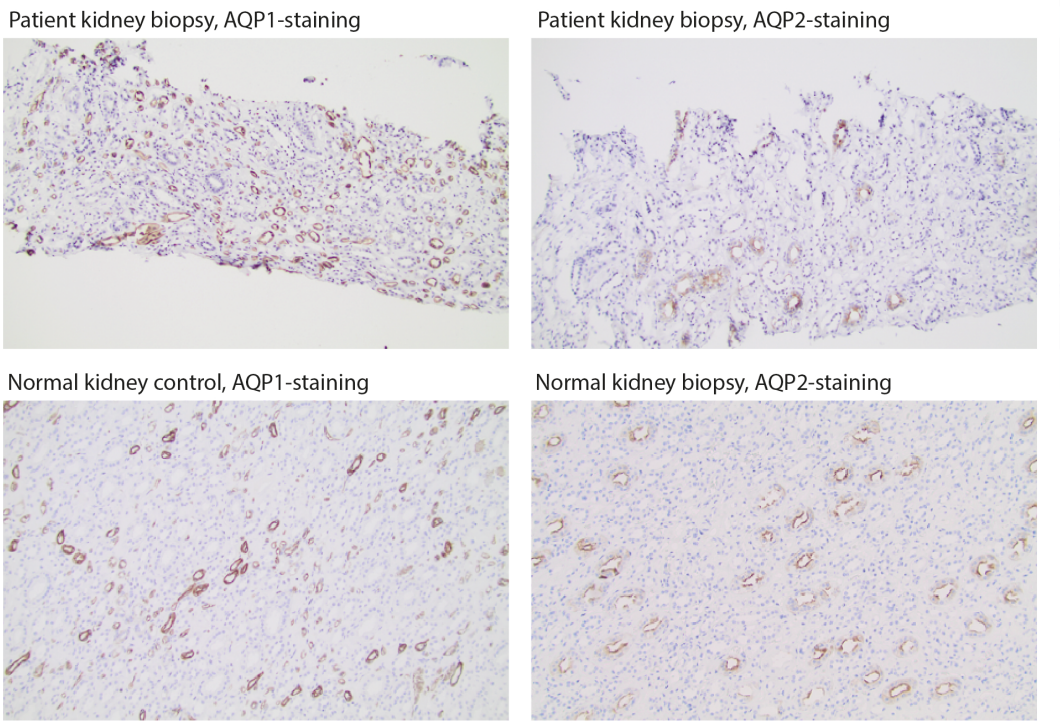

Fig. S1. Kidney tissue pathology. To better define which parts of the tubular system that showed the most pronounced atrophy, we

performed immunohistochemistry using markers for different tubular segments. Anti-AQP1 was used to label the proximal tubules, the long descending thin limbs of Henle's loop and the descending vasa recta, whereas anti-AQP2 was used to identify the collecting duct system principal cells and the cortical and the medullary collecting tubule. The kidney tissue sample from *Patient 2* was compared against healthy kidney tissue. Tubular atrophy was seen throughout the tubular system and appeared to more pronounced in the collecting ducts compared to the proximal tubules.

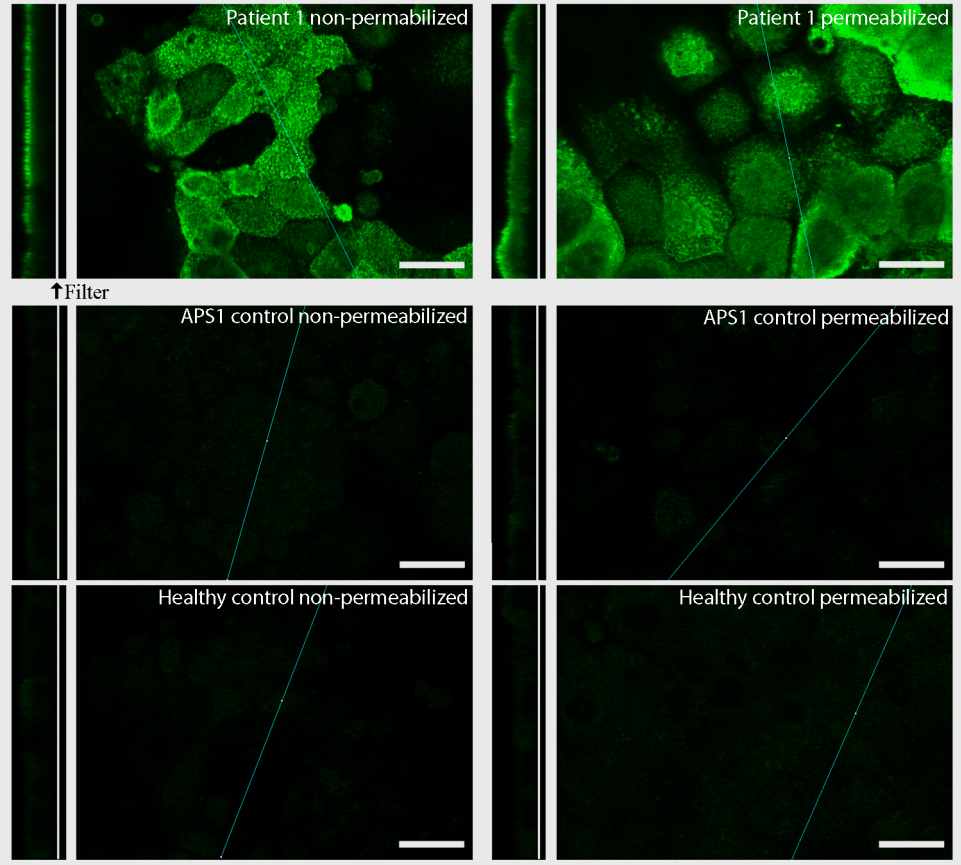

Fig. S2. Immunocytochemistry and confocal laser scanning microscopy of mouse collecting duct principal cells.

mpkCCD#11 cells were grown on permeable supports to stimulate native expression of AQP2. Filters were labeled with patient or control sera either under non-permeabilized or permeabilized conditions. Representative confocal laser scanning images are shown in both X-Y and X-Z (yellow line represents z-section) projections. Serum from *Patient 1* labeled cells under both conditions, indicating that the autoantibody reacted with an external epitope on AQP2. Sparse labeling was observed for serum from *Patient 1* in cells grown in the

absence of vasopressin (not shown). Scale bar = 25μm in all panels, except *Patient 1* permeabilized = 20μm.

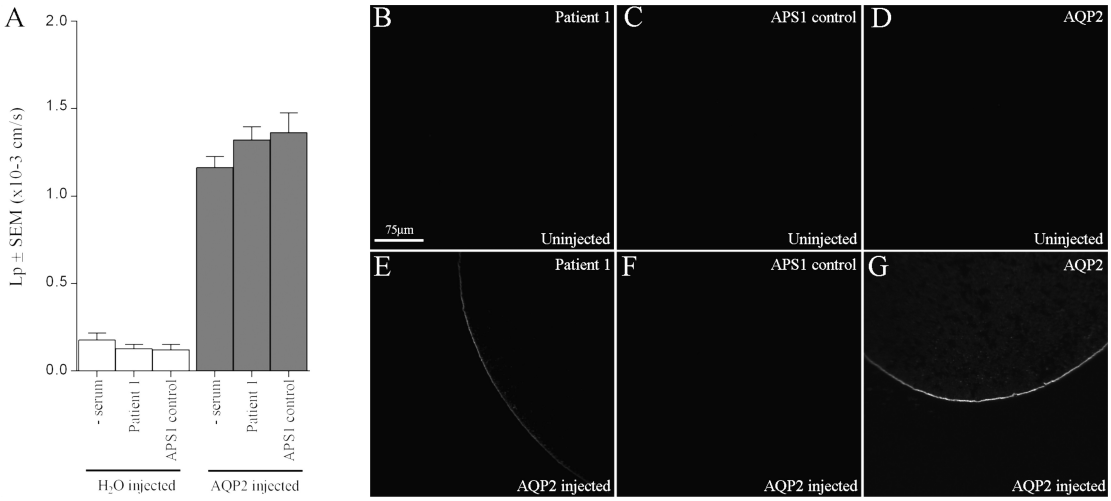

Fig. S3. No significant effects of AQP2 autoantibodies on water permeability.

Oocytes injected with human AQP2 cDNA and uninjected control oocytes were incubated for 72 h. During the last 18 h some oocytes were incubated with patient sera as indicated. A) Summary data of oocyte water permeability (n = 5 oocytes per experiment, 3 experiments). AQP2 injected oocytes displayed significantly higher water permeability relative to control oocytes, but no significant differences were observed following incubation with various patient sera. B-G) Representative laser-scanning confocal images of

representative oocytes following addition of secondary antibody alone (n = 2–3 oocytes per experiment). Labeling of the oocyte plasma membrane was observed only in *Patient 1* sera incubated AQP2 expressing oocytes (E). Standard immunocytochemical labeling using an AQP2 antibody was used as a positive control (G).

APS1 patients	Collecting duct autoantibodies (IF)	cDNA library immunoscreen	RLBA
Patient 1	Detected	Not performed	AQP2
Patient 2	Detected	12 clones isolated, 10 corresponding to *HOXB7*, 2 corresponding to *HOXB2*	HOXB7
Patient 3	Detected	3 clones isolated, 2 corresponding to *NFAT5*, 1 corresponding to *BRAP*	Not performed

Table S2. Characterization of collecting duct autoantibodies.

Autoantibodies against renal collecting duct cells were detected in sera from the three patients with tubulointerstitial nephritis by indirect immunofluorescence (IF) on kidney sections. Autoantibodies against AQP2, HOXB7 and NFAT5 were demonstrated by immunoscreening a

collecting duct cDNA library and by using radio-ligand binding assays (RLBA).

Transcription factor binding site analyses of the AQP2 promoter

Several conserved TFBS were demonstrated (Figure S6), including V$HOXF and V$NFAT. In Figure S7, the following solution parameters were used to visualize the conformity between species and the TREBs position relative to the transcription start: General Core Promoter Elements (0.75/Optimized) and Vertebrates (0.75/Optimized), minimum number of sequences 6/7, distance between elements 5-200, distance variation 100, elements in model 2-10. MatrixSimilarity was set to 0.02 and no. sequences to 1. The figures are showing TFBS in models with 8 elements.

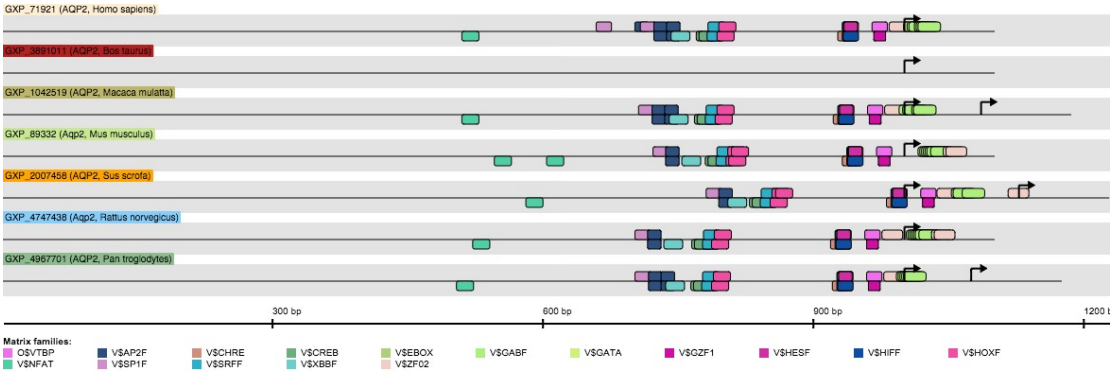

Fig. S4. Analysis of transcription factor binding sites in the human AQP2 promoter region. 1000 bp upstream of the first exon was analyzed with tools from the Genomatix software suite. Binding sites for the following transcription factors and transcription factor families were identified: Vertebrate TATA binding protein factor (O$VTBP), Activator protein 2 (V$APF2), Carbohydrate response elements, consist of two E box motifs separated by 5 bp (V$CHRE), cAMP-responsive element binding proteins (V$CREB), E-box binding factors (V$EBOX), GA-boxes (V$GABF), GATA binding factors (V$GATA), GDNF-inducible zinc finger gene 1 (V$GZF1), Vertebrate homologues of enhancer of split complex (V$HESF), Hypoxia inducible factor, bHLH/PAS protein family (V$HIFF), Paralog hox genes 1-8 from the four Hox clusters A, B, C, D (V$HOXF), Nuclear factor of activated T-cells (V$NFAT), GC-Box factors SP1/GC (V$SP1F), Serum response

element binding factor (V$SRFF), X-box binding factors (V$XBBF), C2H2 zinc finger transcription factors 2 (V$ZF02).

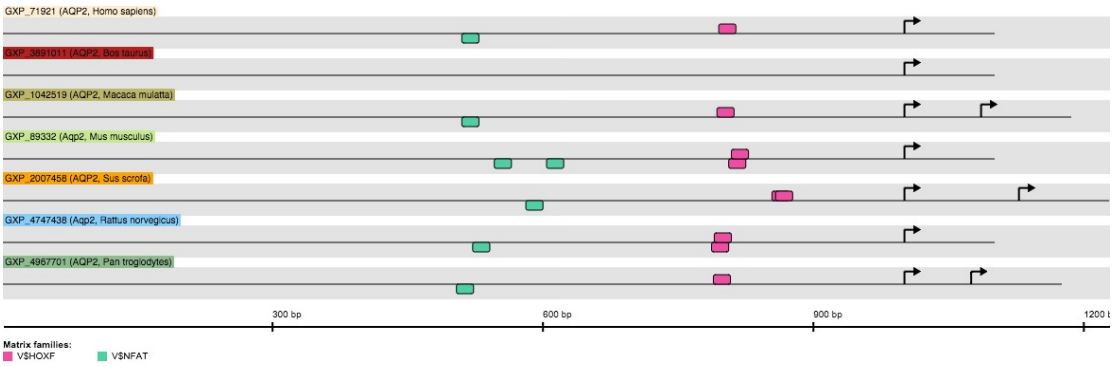

Fig. S5. Analysis of binding sites for NFAT and HOX in the human AQP2 promoter region. 1000 bp upstream of the first exon was analyzed with tools from the Genomatix software suite. Transcription factor binding sites for Paralog hox genes 1-8 from the four Hox clusters A, B, C, D (V$HOXF) and Nuclear factor of activated T-cells (V$NFAT) were identified in *Homo sapiens, Macaca mulatta, Pan troglodytes, Mus musculus, Rattus norvegicus* and *Sus scrofa*.

REFERENCES

1. Yu M-J, Miller RL, Uawithya P, et al. Systems-level analysis of cell-specific AQP2 gene expression in renal collecting duct. Proc Natl Acad Sci U S A 2009;106:2441-6.
2. Moeller HB, Aroankins TS, Slengerik-Hansen J, Pisitkun T, Fenton RA. Phosphorylation and ubiquitylation are opposing processes that regulate endocytosis of the water channel aquaporin-2. Journal of cell science 2014;127:3174-83.
3. Moeller HB, MacAulay N, Knepper MA, Fenton RA. Role of multiple phosphorylation sites in the COOH-terminal tail of aquaporin-2 for water transport: evidence against channel gating. American journal of physiology Renal physiology 2009;296:F649-57.
4. Stokes JB, Grupp C, Kinne RK. Purification of rat papillary collecting duct cells: functional and metabolic assessment. Am J Physiol 1987;253:F251-62.
5. Rorsman F, Husebye ES, Winqvist O, Bjork E, Karlsson FA, Kampe O. Aromatic-L-amino-acid decarboxylase, a pyridoxal phosphate-dependent enzyme, is a beta-cell autoantigen. Proc Natl Acad Sci U S A 1995;92:8626-9.